Probe molecules in polymer melts near the glass transition: A molecular dynamics study of chain length effects

ARTICLE *in* THE JOURNAL OF CHEMICAL PHYSICS · JANUARY 2010

Impact Factor: 2.95 · DOI: 10.1063/1.3284780 · Source: PubMed

3 AUTHORS:

Renaud Arthur Vallée
French National Centre for Scientific Research
87 PUBLICATIONS **1,423** CITATIONS

SEE PROFILE

Wolfgang Paul
Martin Luther University Halle-Wittenberg
183 PUBLICATIONS **5,449** CITATIONS

SEE PROFILE

Kurt Binder
Johannes Gutenberg-Universität Mainz
1,065 PUBLICATIONS **45,231** CITATIONS

SEE PROFILE

Probe molecules in polymer melts near the glass transition: A molecular dynamics study of chain length effects

R. A. L. Vallée,[1] W. Paul,[2,a)] and K. Binder[3]
[1]*Centre de Recherche Paul Pascal (CNRS), 115 Avenue du Docteur Albert Schweitzer, 33600 Pessac, France*
[2]*Institut für Physik, Martin-Luther-University, 06099 Halle, Germany*
[3]*Institut für Physik, Johannes-Gutenberg University, 55099 Mainz, Germany*

(Received 5 October 2009; accepted 11 December 2009; published online 15 January 2010)

Molecular dynamics simulations of a dense melt of short bead-spring polymer chains containing $N=5$, 10, or 25 effective monomers are presented and analyzed. Parts of our simulations include also a single dumbbell ($N=2$) of the same type, which is interpreted to represent a coarse-grained model for a fluorescent probe molecule as used in corresponding experiments. We obtain the mean-square displacements of monomers and chains center of mass, and intermediate incoherent scattering functions of both monomers in the chains and particles in the dumbbells as function of time for a broad regime of temperatures above the critical temperature T_c of mode-coupling theory. For both the chains and the dumbbell, also orientational autocorrelation functions are calculated and for the dumbbell time series for the time evolution of linear dichroism and its autocorrelation function are studied. From both sets of data we find that both the mode-coupling critical temperature T_c (representing the "cage effect") and the Vogel–Fulcher temperature T_0 (representing the caloric glass transition temperature) systematically increase with chain length. Furthermore, the dumbbell dynamics yields detailed information on the differences in the matrix dynamics that are caused by the chain length variation. Deviations from the Stokes–Einstein relation are discussed, and an outlook to related experiments is given. © *2010 American Institute of Physics*.
[doi:10.1063/1.3284780]

I. INTRODUCTION

Polymer melts are very well suited for experimental studies[1–4] of the slowing down of the dynamics when one approaches the glass transition: The free energy barriers against crystallization from the random coil state in supercooled melts are extremely high,[2,5] and hence very slow cooling protocols can be applied, without encountering the problem that formation of crystalline nuclei spoils the results. Moreover, a wealth of experimental techniques to explore the dynamics of the polymer coils is available,[1,2] including also the possibility of adding a small fraction of small molecule probes[6–21] that explore the heterogeneous environment[22–24] in such systems near the glass transition, without creating too much disturbance to these environments.[25–27] In this paper, we shall emphasize another important advantage of flexible macromolecules: One can vary the degree of polymerization (henceforth referred to as "chain length") without changing the intermolecular forces.[28] Thus characteristics such as the size of the polymer coils, the configurational entropy in the system, the diffusion constant of the coils, etc., are changed[2,28,29] but interactions among the monomeric groups (which act as the driving force for the densification of the melt when the temperature is lowered and hence are ultimately responsible for the glass-like freezing which results) stay unaffected. The presence of such an additional control parameter that can be changed without affecting the "chemistry" of the system is a valuable tool for testing the validity of theoretical concepts.[3,4] In fact, the early experimental finding[30] that the glass transition temperature $T_g(N)$ varies with chain length N as

$$T_g(N) = T_g(\infty)(1 - \text{const}/N) \tag{1}$$

has found considerable attention; in particular Eq. (1) was also obtained from, the "entropy theory" proposed by Gibbs and di Marzio[31] (suggesting that the glass transition of polymer melts results from the vanishing of their configurational entropy, a concept motivated[32] by Kauzmann's observation that for many glass forming fluids the extrapolation of their calorimetric entropy data falls below the crystal entropy at a nonzero temperature T_K, the "Kauzmann temperature"). We now know that the experimental validity of Eq. (1) is not a sufficient proof to claim the validity of the "entropy catastrophe" concept of Gibbs and di Marzio;[31] in fact, unjustifiable approximations in their treatment are well documented.[33,34] Moreover, there is no thermodynamic principle that forbids the entropy of a supercooled fluid to fall below the entropy of a crystal (in fact, this is known to happen for a very simple model system, the fluid of hard spheres).[35]

Nevertheless, it is of significant interest to explore in detail the effects of varying the chain length N on the slow dynamics near the glass transition, and thus gain better insight into its properties. In the present work, we contribute to this problem by presenting molecular dynamics (MD) results for a simple model system, a melt of simple bead-spring

a)Electronic mail: wolfgang.paul@physik.uni-halle.de.

chains, varying N in the regime where the melts are not yet entangled, $5 \leq N \leq 25$. In previous work, this model has been extensively characterized, but for a single chain length ($N=10$) only.[36–44] Since in recent work[25–27] it was shown that useful complementary information can be extracted when one includes a dumbbell molecule [which can be regarded as a coarse-grained description of fluorescent probe molecules[25–27] which have yielded a wealth of information in single molecule spectroscopy (SMS) experiments[6–20]], we perform additional simulations where a dumbbell ($N=2$) is included in the simulations in the present case as well. As shown previously,[25–27] the study of the slow translational and rotational dynamics of this probe in the glass forming fluid environment yields information on the energy landscape of the system.[45–53] Since in the course of its motion the dumbbell probes regions of different local structures and mobilities, it is clear that analysis of this motion gives very direct information on the dynamic heterogeneity in the supercooled melt. Moreover, also the dynamics of transitions from one "metabasin"[48–51] in the energy landscape to the other[54] can be elucidated as we have shown.[25–27]

In Sec. II, we briefly recall the model and simulation method, while in Sec. III we present results on the intermediate incoherent dynamic structure factors and mean-square displacements. Also orientational correlation functions are explored, which would be experimentally accessible for fluorescent probe molecules. These results are analyzed within the framework of idealized mode-coupling theory[55] (MCT) to test to what extent the critical temperature T_c of MCT actually depends on chain length N. Since our data are restricted to the temperature range $T/T_c - 1 \geq 0.04$, the fact that the singularities predicted by the idealized MCT at T_c are actually rounded off does not affect our analysis. We obtain both the relaxation time τ_q for "α-relaxation"[1–5,56,57] and the self-diffusion constant D and also address the question whether the Stokes–Einstein relation $D\tau_q/T=\text{const}$ holds in this regime.

In Sec. IV we present a tentative brief discussion whether an alternative analysis of the same data in terms of fits to the Vogel–Fulcher relation[58] leads to a chain length dependence of the Vogel–Fulcher temperature T_0. Section V then presents some discussion of trajectories $d(t)$ that would correspond to the linear dichroism of a fluorescent probe molecule, and the resulting correlation function, while Sec. VI briefly summarizes our conclusions.

II. METHODS

We performed MD simulations of a system containing either 240, 120, or 48 bead-spring chains of 5, 10, or 25, respectively, effective monomers. A cubic simulation volume with periodic boundary conditions is used throughout. The interaction between two beads of type A (probe) or type B (monomers) is given by the Lennard-Jones (LJ) potential $U_{\mathrm{LJ}}(r_{ij})=4\epsilon[(\sigma_{\alpha\beta}/r_{ij})^{12}-(\sigma_{\alpha\beta}/r_{ij})^{6}]$, where r_{ij} is the distance between beads i,j and $\alpha,\beta \in A,B$. The LJ diameters used are $\sigma_{AA}=1.22$, $\sigma_{BB}=1.0$ (unit of length), and $\sigma_{AB}=1.11$, while $\epsilon=1$ sets the scale of energy (and temperature T since Boltzmann's constant $k_B=1$). These potentials are truncated at $r_{\mathrm{cut}}^{\alpha\beta}=2^{7/6}\sigma_{\alpha\beta}$ and shifted so that they are zero at $r_{ij}=r_{\mathrm{cut}}^{\alpha\beta}$. Between the beads along the chain, as well as between the beads of the dumbbell, a finitely extendable nonlinear elastic potential is used $U_F=-(k/2)R_0^2\ln[1-(r_{ij}/R_0)^2]$, with parameters $k=30$ and $R_0=1.5$.[36] This model system (without the probe) has been shown to qualitatively reproduce many features of the relaxation of glass forming polymers.[36–44] In the MD simulations, the equations of motion at constant particle number N, volume V, and energy E are integrated with the velocity Verlet algorithm[59,60] with a time step of 0.002, measuring time in units of $(m_B\sigma_{BB}^2/48\epsilon)^{1/2}$. All NVE simulations have been performed after equilibrating the system in the NpT ensemble, using a Nosé–Hoover thermostat,[60] keeping the average pressure at $p=1.0$ at all temperatures. These runs lasted up to 5×10^7 MD steps. Ten different configurations were simulated at each temperature ($T=0.47, 0.48, 0.49, 0.5, 0.55, 0.6, 0.65, 0.7, 1.0, 2.0$) in order to ensure good statistics. Note that the melting temperature of the crystalline phase of this model polymer has been estimated[42] to be $T_m=0.75$ while the critical temperature T_c of MCT (where in our model a smooth crossover to activated dynamics occurs) is at $T_c=0.45$ (Refs. 36–42) (both values were obtained for chains of length $N=10$). Thus our data include equilibrated melts as well as the moderately supercooled regime.

III. RESULTS FOR THE INTERMEDIATE STRUCTURE FACTOR AND MEAN SQUARE DISPLACEMENTS: MODE COUPLING ANALYSIS

A. Pure melts

Previous experience[31,36–40,42–44] has shown that a quantity that is particularly useful to analyze the slow dynamics of glass forming liquids in the context of theory and simulations is the incoherent intermediate scattering function $F_q(t)$,

$$F_q(t) = \frac{1}{M}\sum_{i=1}^{M} \langle \exp[i\vec{q}\cdot(\vec{r}_i(0)-\vec{r}_i(t))]\rangle. \tag{2}$$

In Eq. (2), the sum is extended over all M effective monomers in the system, and $\vec{r}_i(t)$ is the position of the ith monomer at time t, while $\vec{q}$ is the scattering wave vector. The angular brackets indicate a thermal as well as an orientational average. Being interested in the slow dynamics associated with the cage effect,[3,4,55] it is most useful to choose q such that it roughly corresponds to the position where the static structure factor $S(q)$ of the melt has its peak, which is (for the chosen conditions) $q=6.9$ [note that in the temperature regime of interest, $S(q)$ changes with temperature only very little[3,36]]. Of course, an analogous quantity can be immediately defined for the dumbbell if the simulated system contains one; the only problem then is that due to the small number $M=2$ (rather than $M=1200$), the poor statistics necessitates to carry out multiple runs (as mentioned in Sec. II, ten independent runs were hence performed).

As an example of our results for pure systems (without dumbbell) and their analysis, we present $F_q(t)$ for $N=5$ versus the scaled time, t/τ_q, where the α-relation time τ_q is defined by the condition

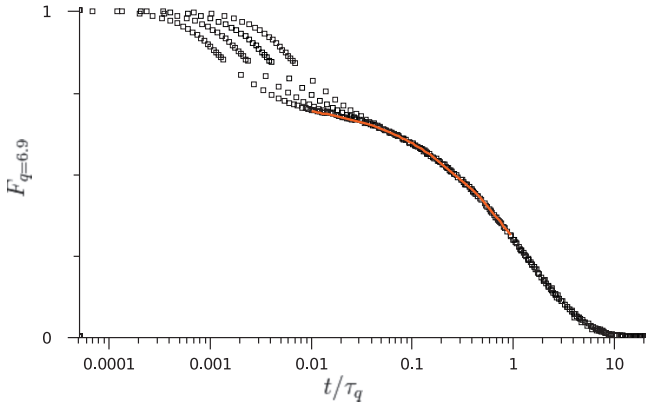

FIG. 1. Intermediate dynamic structure factor (black open squares) for the model system of chains with five monomers. Time is scaled by the α-relaxation time τ_q for the four lowest investigated temperatures $T=0.47$,0.48, 0.49, and 0.50 (from left to right), where the time-temperature superposition principle notably holds. Also shown (red curve) is the best fit $F_q(t)=f_q^c-h_q(t/\tau_\alpha)^b+h_qB_q(t/\tau_\alpha)^{2b}$ performed simultaneously to these four curves (see text).

$$F_{q=6.9}(t=\tau_q)=0.3. \tag{3}$$

Figure 1 shows that in this temperature range $0.47 \leqq T \leqq 0.50$ $F_q(t)$ has a two-step decay, and the second step [the decay of $F_q(t)$ from about $F_q(t)=0.5$ to zero] displays the expected[3,4,55,56] time-temperature superposition principle very well. We have also checked that a different convention, such as defining τ_q via $F_{q=6.9}(t=\tau_q)=0.1$, only would lead to a change in τ_q by a constant factor, but would not affect our results.

We will analyze the incoherent scattering function in Fig. 1 following a simplified procedure compared to the more elaborate analysis presented in Ref. 43. The first step of the decay seen in Fig. 1 ("critical decay"[3,4,55,56]) leads to a plateau (described by the "nonergodicity parameter" f_q^c), and will not be analyzed in detail here. However we are interested in the decay of the plateau, which according to MCT (Ref. 55) can be described in the β-relaxation regime by (f_q^c, h_q, B_q, and b are fitting parameters)

$$F_q(t)=f_q^c-h_q(t/\tau_\alpha)^b+h_qB_q(t/\tau_\alpha)^{2b}+-\cdots. \tag{4}$$

From a simultaneous fit of Eq. (4) to the four curves corresponding to the four lowest temperatures investigated here, notably $T=0.47$, $T=0.48$, $T=0.49$, and $T=0.5$, the MCT parameter $b\approx 0.57$ is extracted. MCT exponent relations then fix the exponent of the α-relaxation in the law

$$\tau_{q=6.9}(T) \propto (T/T_c(N)-1)^{-\gamma} \tag{5}$$

to $\gamma=2.5$. This law implies that a plot of $(\tau_{q=6.9})^{-1/\gamma}$ versus T should be linear and intersect zero at $T_c(N)$. Figure 2 shows that in the temperature regime $0.47 \leq T \leq 0.65$ used for these fits good straight lines are in fact obtained [with $T_c \simeq 0.42 \pm 0.02$ and $\gamma \approx 2.64$ for $N=5$ (which agrees reasonably with the expectation according to the MCT exponent relations), while within our accuracy the estimates for $T_c(N)$ for $N=10$ and $N=25$ coincide, $T_c(N \geq 10)=0.45 \pm 0.02$]. The error bars are conservative to account for the fact that our simplified analysis obtains $T_c(N)$ and $\gamma(N)$ from just one fit. A full MCT analysis with a simultaneous fit of several quantities in the α- and β-relaxation regimes is beyond the scope of this manuscript and will be presented in future work.

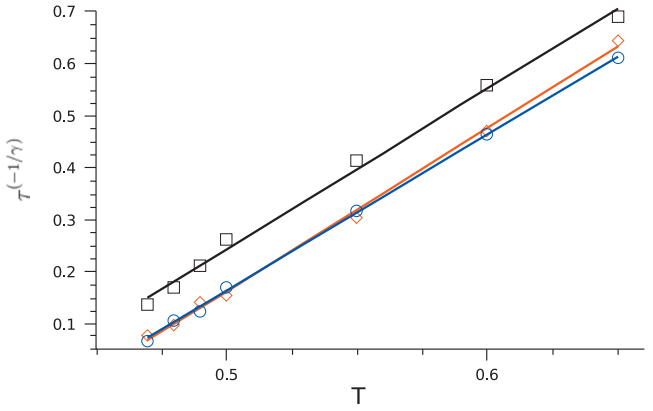

FIG. 2. Critical behavior of the α-relaxation time scale as a function of temperature, allowing for a determination of the critical temperature T_c. Black squares, red diamonds, and blue circles give the α-relaxation times as a function of temperature for chains with lengths of 5, 10, and 25, respectively. The solid curves of corresponding color provide the best fits (MCT power law divergence) to the data, allowing for the determination of $T_c=0.42$ in the case of chain lengths of five monomers and $T_c=0.45$ in the case of chain lengths of 10 and 25 monomers. The α-relaxation times have been determined empirically in this case by the requirement $F_q(\tau_q)=0.3$. The same analysis performed by defining empirically the α-relaxation times with the requirement $F_q(\tau_q)=0.1$ provides the same estimates for $T_c(N)$.

The cage effect which MCT captures originates in the dense packing of the molecules. As we are studying the glass transition along an isobar, the variation of $T_c(N)$ with chain length has to be at least partly due to the variation of density with chain length at fixed temperature along the isobar. In fact, in our earlier work[39] we found an increase in T_c at fixed chain length ($N=10$) with increasing pressure, i.e., increasing density at fixed temperature. In Fig. 3 we show the density variation with temperature in our three simulated melts. In the displayed temperature regime, the densities vary linearly with chain length according to $\rho_5(T)=1.153-0.268$ T, $\rho_{10}(T)=1.172-0.279$ T, and $\rho_{25}(T)=1.172-0.264$ T. This yields densities at T_c of $\rho_5(T_c)=1.040$, $\rho_{10}(T_c)=1.046$, and $\rho_{25}(T_c)=1.053$. Within our analysis we therefore find a slight increase in the critical density with chain length, presumably due to connectivity influences on the cage effect in a polymer melt.

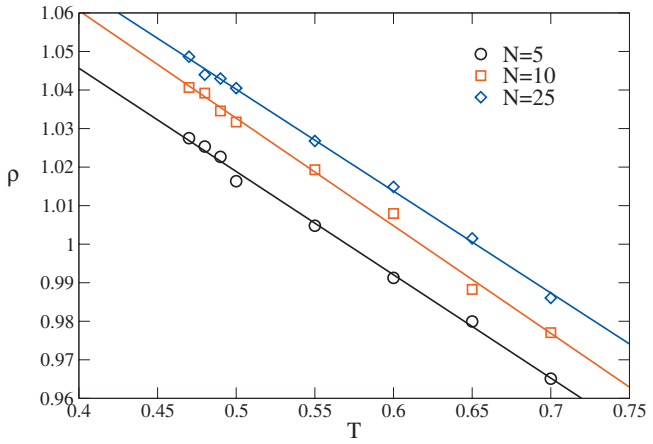

FIG. 3. Density variation along the $p=1$ isobar for the three chain lengths studied. In the displayed temperature regime, the density variation is linear as shown by the regression lines (see text).

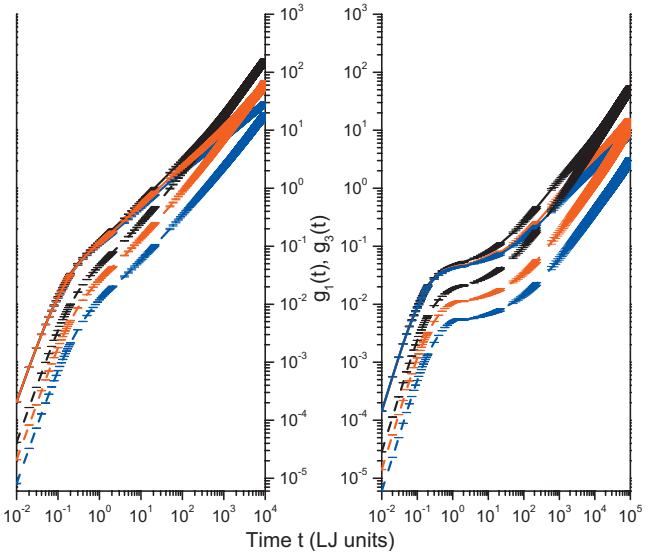

FIG. 4. Mean square displacements as a function of time for $T=0.7$ (left) and $T=0.48$ (right). g_1 (solid curves) and g_3 (dashed curves) describe the monomers and the center of mass of the chains, respectively. The black, red, and blue curves pertain to chains with lengths of 5, 10, and 25 monomers in the simulation boxes.

The second quantity that we analyze is mean-square displacements of individual effective monomers,

$$g_1(t) \equiv \frac{1}{M}\sum_{i=1}^{M} \langle [\vec{r}_i(t) - \vec{r}_i(0)]^2 \rangle \tag{6}$$

and of the center of mass of the chains ($n=M/N$)

$$g_3(t) = \frac{1}{n}\sum_{j=1}^{n} \langle [\vec{r}_{CM,j}(t) - \vec{r}_{CM,j}(0)]^2 \rangle, \tag{7}$$

where the sum in Eq. (6) runs over all monomers and the sum in Eq. (7) runs over all chains, $\vec{r}_{CM,j}(t)$ being the position of the center of mass of the jth chain. These quantities are shown in Fig. 4 for two representative temperatures and all three chain lengths investigated. For the high temperature ($T=0.7$) the center of mass motion after an initial "ballistic" regime[3] crosses over to a slightly subdiffusive regime $\simeq t^{0.8}$ (see Ref. 61) and then to standard diffusive motion, D_t being the translational diffusion coefficient,

$$g_3(t) = 6D_t t. \tag{8}$$

At the lower temperature ($T=0.48$), however, there is a clear plateau due to the cage effect. For $g_1(t)$ the displacements in the ballistic regime are larger than $g_3(t)$ by a factor of N, as it must be, and there occurs a regime of subdiffusive growth [ideally, there should be Rouse-like behavior $g_1(t) \propto t^{1/2}$] before $g_1(t)$ and $g_3(t)$ merge, and also $g_1(t)$ shows the expected diffusive behavior, $g_1(t)=6D_t t$. At the lower temperatures, where the cage effect comes into play, $g_1(t)$ displays a pronounced plateau after the ballistic regime, and the escape from the plateau also involves another power law [accounted for by MCT (Refs. 3 and 41)], but this shall not be further discussed here. From the Fickian diffusion regime reached for g_3 for times larger than the Rouse time, estimates for the translation diffusion constants D_t have been extracted. Again

TABLE I. Parameters obtained by fitting the MCT law to α relaxation times τ_q, τ_2, and τ_4 and to the translational diffusion coefficients D_t for the model systems with chains of either 5, 10, or 25 monomers. Results of fits obtained by fixing the critical temperature to the known value for each polymer model (Fig. 4).

	τ_x					
Bulk	T_c (5)	γ (5)	T_c (10)	γ (10)	T_c (25)	γ (25)
τ_q	0.42	2.64	0.45	2.19	0.45	2.44
τ_2	0.42	2.24	0.45	1.87	0.45	2.21
τ_4	0.42	2.64	0.45	2.22	0.45	2.55
D_t	0.42	2.24	0.45	1.77	0.45	1.93
Dumbbell	T_c (5)	γ (5)	T_c (10)	γ (10)	T_c (25)	γ (25)
τ_q	0.42	2.72	0.45	2.23	0.45	2.51
τ_2	0.42	2.41	0.45	2.08	0.45	2.18
τ_4	0.42	2.71	0.45	2.23	0.45	2.49
D_t	0.42	2.45	0.45	1.90	0.45	2.03

one expects from the idealized MCT (Ref. 55) a power law as in Eq. (5),

$$D_t \propto (T/T_c(N) - 1)^{\gamma}. \tag{9}$$

The various estimates both for $T_c(N)$ and for γ, including those extracted from the dumbbell (see Sec. III B) are collected in Table I. As already found in our earlier work for $N=10$,[36] the exponent estimate γ extracted from D_t is distinctly smaller than the estimate from $\tau_{q=6.9}$. MCT (Ref. 55) implies that asymptotically close to $T_c(N)$, the exponents γ appearing in Eqs. (5) and (9) should be the same. The discrepancy between both estimates may be due to the fact that our data are not close enough to $T_c(N)$; on the other hand, the singularities predicted by the idealized MCT anyway are rounded off, and hence the true asymptotic region of idealized MCT may not be observable in our system. In addition to this problem, Table I also implies that the exponent(s) γ may depend on chain length.

B. Melts containing a dumbbell

As mentioned above, it is straightforward to obtain $F_{q=6.9}(t)$ for the dumbbell as well. Figure 5 compares the resulting data with those of the chains at two temperatures. One can see that the function $F_{q=6.9}(t)$ is very similar to the corresponding function of the melt (the decorrelation of the dumbbell always is a bit slower due to the choice of the larger ranges of the potentials σ_{AA}, σ_{AB}, chosen for the two monomers in the dumbbell). In spite of the small difference between the time scale for α-relaxation of the dumbbell and the melts in which it moves, one can infer from dumbbell data alone how much additional slowing down occurs when N is increased. Thus we conclude from Fig. 5 that SMS studies of probe dynamics can yield valuable information on subtle differences between different matrices in which the probe is embedded, at least for temperatures above and close to T_c.

It is also very interesting to explore the rotational dynamics of the probe.[25–27] Defining $\vec{u}(t)$ as a unit vector along

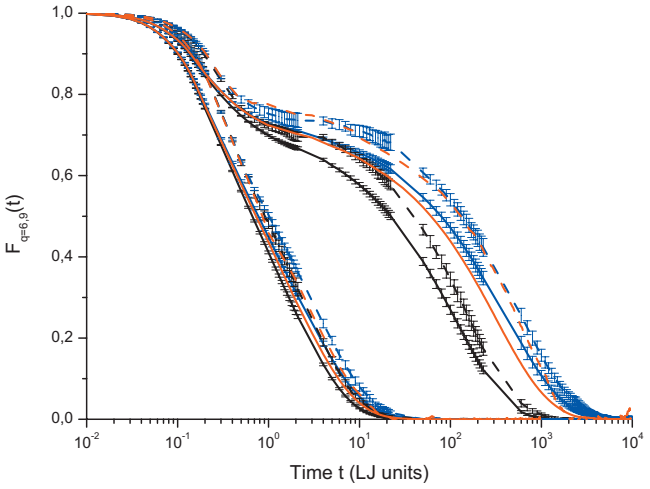

FIG. 5. Intermediate dynamic structure factor at the first maximum ($q=6.9$) of the static structure factor for the NVE simulations performed at temperatures $T=0.7$ (left) and $T=0.48$ (right) for various chain lengths. Black, red, and blue curves represent the results for chains of 5, 10, and 25 monomers in the simulation boxes, respectively. Dashed curves stand for the probe (dumbbell) dynamics while solid curves stand for the bulk dynamics. The error bars, estimated by the Jackknife approach on the base of the ten simulation runs for each temperature, are obviously larger for the dumbbell dynamics than for the bulk dynamics.

the axis connecting the positions of the two particles in the dumbbell at time t, it is useful to define orientational time correlation functions in terms of

$$\cos(\theta(t)) = \vec{u}(t) \cdot \vec{u}(0) \tag{10}$$

via the Legendre polynomials $P_\ell(\cos\theta)$ as

$$C_\ell(t) \equiv \langle P_\ell(\cos\theta(t)) \rangle \tag{11}$$

and corresponding relaxation times $\tau_\ell = \int_0^\infty C_\ell(t)dt$. As discussed previously,[26,27] the relaxation times τ_2 and τ_4 are of particular interest, and are included in Table I. Here we have included also data for the orientational correlations of bonds in the polymer chain, which can be defined analogously (averaging the data over all bonds in all polymers, irrespective of whether a monomer is at a chain end or not).

Figures 6 and 7 then present the various relaxation times τ_q, τ_2, and τ_4 on a log-log plot versus $T-T_c(N)$, both for the bulk (i.e., monomers of the melt) and the dumbbell. It is seen that the simple power law is only a rough description of the data, but the latter clearly suffers from some statistical errors, in particular, in the case of the dumbbells. The resulting exponents γ (which are estimated from the slopes of this plot) are collected in Table I. The exponents of τ_q and τ_4 always are very similar because they probe motions on the same scale, as already noted in Ref. 27. The exponent of τ_2 agrees with the exponent of D_t in the case of $N=5$, while in the case of $N=25$ the exponent of D_t is clearly smaller. If this result is not an artifact of insufficient statistics, the argument could be that the diffusion constant is related to a scale of the order of the coil size, which is clearly larger than the bond length for $N=25$, but not for $N=5$. However, we add the caveat that a log-log plot of the diffusion constant versus $T-T_c(N)$, Fig. 8, exhibits inevitably pronounced scatter for the dumbbell, and hence these data have to be considered with caution.

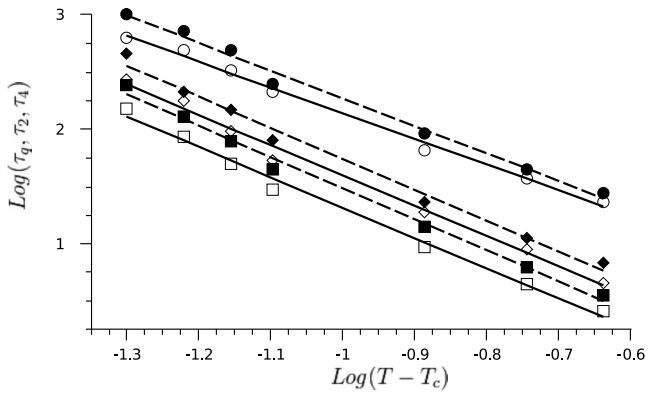

FIG. 6. Log-log plots of the relaxation times τ_q (squares), τ_2 (circles), and τ_4 (diamonds) for the bulk (open symbols) or the dumbbell (full symbols) in the model system with chains of five monomers. Relaxation times have been determined empirically by requiring a decay of the correlation function to a value of 0.3. The parameters T_c and γ obtained from the fits (solid curve: bulk and dashed curve: dumbbell) to a power law (see text) are given in Table I.

Surprisingly, a somewhat less noisy behavior is obtained if we plot D_t as a function of τ_q/T (Fig. 9): In all cases rather convincing evidence for power law behavior is observed,

$$D_t \propto (\tau_q/T)^{-\xi_t}, \tag{12}$$

the exponent ξ_t being given in Table II. We observe a small but significant deviation of ξ_t from unity, signifying that the breakdown of the Stokes–Einstein relation sets in for $T>T_c$ (but in the supercooled regime) already. For $N=10$, a related finding was already reported in Ref. 27.

IV. AN ATTEMPT TO ESTIMATE THE CHAIN-LENGTH DEPENDENCE OF THE VOGEL–FULCHER TEMPERATURE

As is well known,[3,4] the fit of the α-relaxation time by idealized MCT holds over a rather restricted temperature window only, and an equally good fit often is provided by the Vogel–Fulcher relation,[58] i.e.,

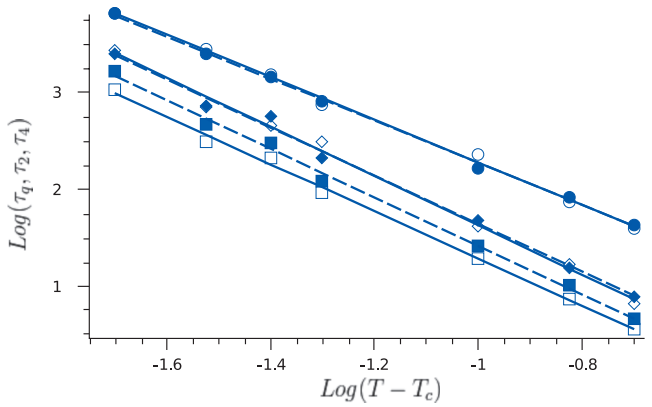

FIG. 7. Log-log plots of the relaxation times τ_q (squares), τ_2 (circles), and τ_4 (diamonds) for the bulk (open symbols) or the dumbbell (full symbols) in the model system with chains of 25 monomers. Relaxation times have been determined empirically by requiring a decay of the correlation function to a value of 0.3. The parameters T_c and γ obtained from the fits (solid curve: bulk and dashed curve: dumbbell) to a power law (see text) are given in Table I.

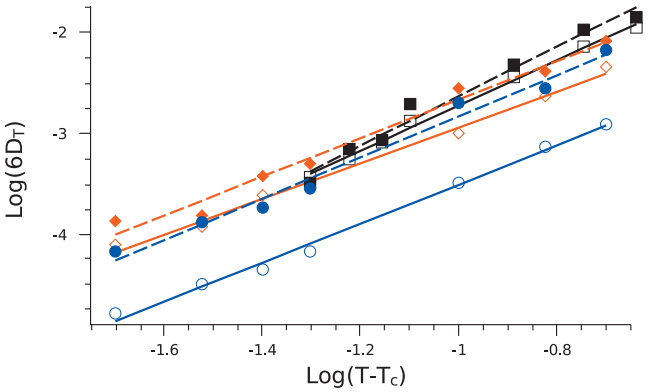

FIG. 8. Log-log plots of the translational diffusion coefficients for the bulk (open symbols) or the dumbbell (full symbols) in the model system with chains of 5 (black squares and curves), 10 (red diamonds and curves), and 25 (blue circles and curves) monomers. The parameters T_c and γ obtained from the fits (solid curve: bulk and dashed curve: dumbbell) to a power law (see text) are given in Table I.

$$\tau = \tau_0(N)\exp[B(N)/(T - T_0(N))], \tag{13}$$

where $\tau_0(N)$ is a prefactor of no interest here, $B(N)$ is some effective activation energy, and $T_0(N)$ is the Vogel–Fulcher temperature. Figures 10 and 11 demonstrate that all our data for $N=5$ and $N=25$ can be nicely fitted by Eq. (13); similar fits for $N=10$ can be found in Ref. 27.

The results of the present fits are collected in Table III, leading to $T_0(N=5) \approx 0.32 \pm 0.03$ while $T_0(N=10) \approx 0.33 \pm 0.04$ (Ref. 27) and $T_0(N=25) \approx 0.37 \pm 0.03$. Plotting these estimates versus $1/N$, as one would expect a straight line from Gibbs–DiMarzio-type arguments, one notes appreciable curvature; however, this is similar to the experimental observations.[30] The three chain length studied therefore do not allow an identification of the exact form of the N-dependence. Performing a tentative extrapolation to $N \to \infty$ employing the Gibbs–DiMarzio prediction would imply $T_0(N \to \infty) \approx 0.38 \pm 0.03$. These estimates suffer, of course, from the fact that they are extrapolated quite some distance below the smallest temperature accessible to us in the simulation. Furthermore, one has to bear in mind that typically the estimate for T_0 decreases when lower temperature data become available, until for temperatures close to the calorimetric glass transition temperature also the Vogel–Fulcher law breaks down.[62] For the results presented in Table III we first determined the best common estimate for $T_0(N)$ and then kept this estimate fixed in the determination of the other parameters. As one would have anticipated, the fits to τ_q and τ_4 lead to comparable values of the activation energy $B(N)$; these observables probe the same type of motion and have comparable relaxation times.[26,27] The second Legendre polynomial of the bond vector (or dumbbell) decays on longer time scales and is more susceptible to collective motion of the environment of the bond (or probe). This is reflected in the reduced value of the activation energy $B(N)$ in Table III as well as in the reduced value of the mode-coupling exponent γ in Table I, which in turn agrees with the exponent for the center of mass diffusion coefficient (zeroth Rouse mode). Relaxation processes on these scales are captured by the Rouse model and were shown to follow the same temperature dependence.[63,64]

TABLE II. Parameters obtained by fitting the fractional functional forms (SE relation modified by ξ_t) to the relaxation times τ_q for either the bulk or dumbbell dynamics in the model systems containing chains of either 5, 10, or 25 monomers.

$$D_T \propto \left(\frac{\tau}{T}\right)^{-\xi_t}$$

	ξ_t (5)	ξ_t (10)	ξ_t (25)
Bulk	0.88	0.85	0.82
Dumbbell	0.89	0.86	0.87

V. LINEAR DICHROISM TRAJECTORIES OF THE PROBE MOLECULES

In many SMS studies, emphasis is placed on the measurement of the linear dichroism trajectories, $d(t)$. In terms of the single molecule emission intensities I_p and I_s along two mutually perpendicular polarization directions, $d(t)$ is defined as

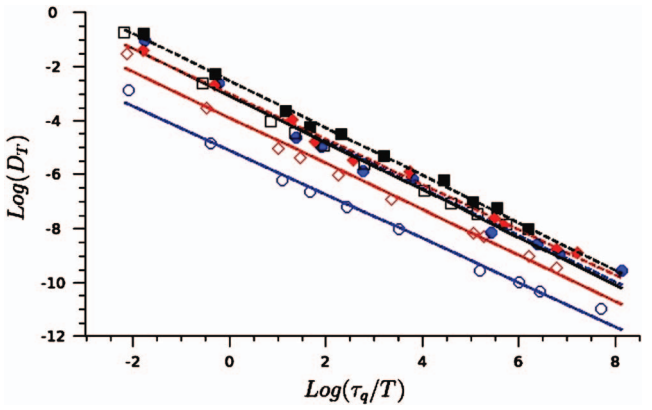

FIG. 9. Power law fits of translational diffusivities D_t as a function of τ_q/T ($q=6.9$): $D_t \approx (\tau_q/T)^{-\xi_t}$ for the bulk (open symbols, solid curves) or the dumbbell (full symbols, dashed curves) in the model system with chains of 5 (black squares and curves), 10 (red diamonds and curves), and 25 (blue circles and curves) monomers. Results for the exponent are given in Table II.

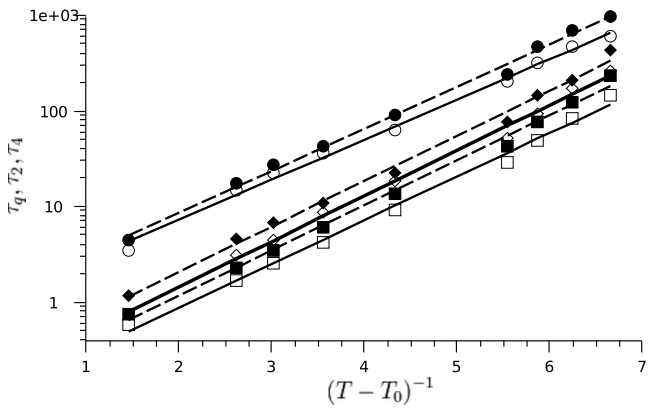

FIG. 10. Vogel–Fulcher plots of the relaxation times τ_q (squares), τ_2 (circles), and τ_4 (diamonds) for the bulk (open symbols, solid curves) or the dumbbell (full symbols, dashed curves) in the model system with chains of five monomers. The values of the Vogel temperature T_0 and of the fragility parameter B/T_0 are presented in Table III.

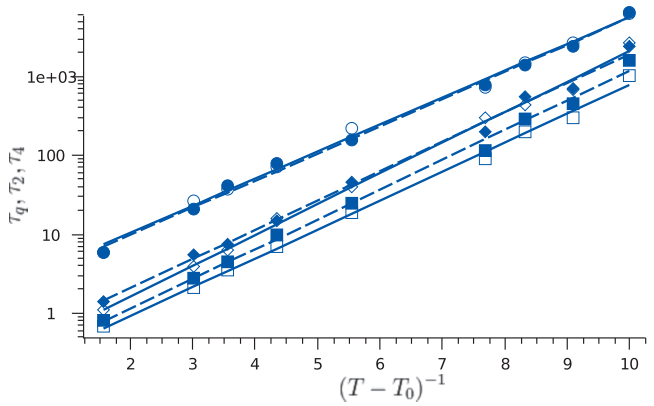

FIG. 11. Vogel–Fulcher plots of the relaxation times τ_q (squares), τ_2 (circles), and τ_4 (diamonds) for the bulk (open symbols, solid curves) or the dumbbell (full symbols, dashed curves) in the model system with chains of 25 monomers. The values of the Vogel temperature T_0 and of the fragility parameter B/T_0 are presented in Table III.

$$d(t) = (I_p - I_s)/(I_p + I_s). \tag{14}$$

In simulations, an equivalent quantity can be defined as[27,65]

$$d(t) = (7/8)[(\vec{e}_1 \cdot \vec{u})^2 - (\vec{e}_2 \cdot \vec{u})^2], \tag{15}$$

where $\vec{e}_1$ and $\vec{e}_2$ are orthogonal unit vectors defining an arbitrary plane intersecting the simulation box and $\vec{u}$ is a unit vector along the dumbbell axis, as before. Figure 12 shows typical raw data of the $d(t)$ trajectory of a dumbbell at $T=0.48$ and the corresponding autocorrelation function. The trajectory exhibits the typical jumps between distinct states, similar as discussed in our earlier work[25–27] for the trajectories of the fluorescence lifetime. The unconventional jumpwise relaxation again can be attributed to the transitions between metabasins in the energy landscape of our model system.[25–27]

TABLE III. Parameters obtained by fitting the Vogel–Fulcher law to α relaxation times τ_q, τ_2, and τ_4 for the model systems with chains of either 5, 10, or 25 monomers. Results of fits obtained by fixing the Vogel temperature to either $T_0=0.32$ (5 monomers), $T_0=0.33$ (10 monomers), or $T_0=0.37$ (25 monomers) are given.

	τ_x					
Bulk	T_0 (5)	B/T_0 (5)	T_0 (10)	B/T_0 (10)	T_0 (25)	B/T_0 (25)
τ_q	0.32	3.29	0.33	3.52	0.37	2.28
τ_2	0.32	3.03	0.33	3.18	0.37	2.13
τ_4	0.32	3.43	0.33	3.63	0.37	2.42
Dumbbell	T_0 (5)	B/T_0 (5)	T_0 (10)	B/T_0 (10)	T_0 (25)	B/T_0 (25)
τ_q	0.32	3.40	0.33	3.60	0.37	2.35
τ_2	0.32	3.18	0.33	3.45	0.37	2.14
τ_4	0.32	3.42	0.33	3.67	0.37	2.31

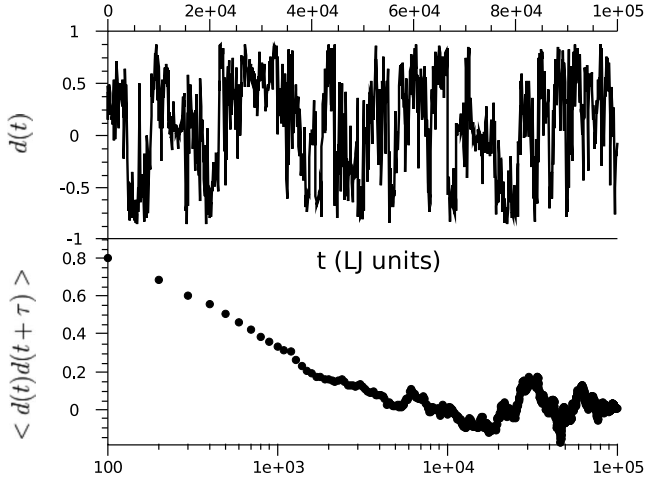

FIG. 12. Linear dichroism $d(t)$ trajectory (top) and corresponding autocorrelation function (bottom) of a dumbbell in a model system with polymer chains of five monomers at a temperature of $T=0.48$.

While the autocorrelation function

$$C_d(\tau) = \langle d(t)d(t+\tau)\rangle \tag{16}$$

shown in Fig. 12 (bottom) corresponds to the single trajectory shown in the top of this figure, one needs to average such data over (at least) ten independent trajectories to get relevant statistics from our simulations. In SMS, the trajectories have been shown to have a required length at least 100 times larger than the typical relaxation times obtained from their time correlation functions in order to ensure a properly built function and a relevant value for the extracted relaxation time.[66] Such averaged data are shown in Fig. 13, where for each temperature again a relaxation time τ_d is extracted requiring $C_d(\tau)=0.3$. The right part illustrates that the time-temperature superposition principle also holds for this quan-

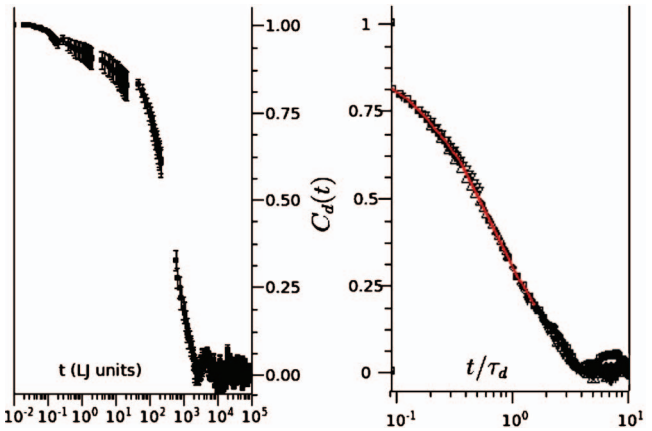

FIG. 13. Left: orientational time correlation function $C_d(\tau)$ (linear dichroism) for the dumbbell in the model system of chains with five monomers at a temperature $T=0.48$. The error bars are estimated by the Jackknife approach on the base of the ten simulation runs at this temperature. Right: time is scaled by the α-relaxation time τ_d of the linear dichroism for the four data sets (black symbols) pertaining to the lowest temperatures investigated in this study $0.47 \leqq T \leqq 0.5$, where the time-temperature superposition principle notably holds. Also shown (red curve) is the best fit $C_d(\tau) = f_d^c - h_d(\tau/\tau_\alpha)^b + h_d B_d(\tau/\tau_\alpha)^{2b}$ performed simultaneously on these four data sets, allowing for the determination of the MCT parameters: $b=0.57$ and $\gamma=2.5$, in agreement with Fig. 1.

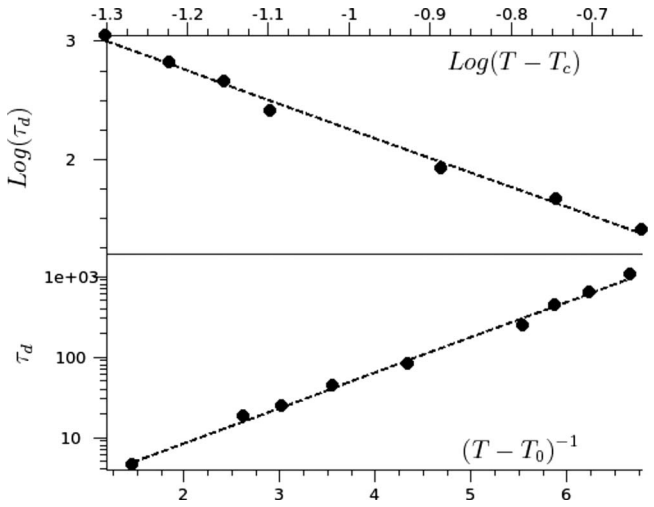

FIG. 14. Top: log-log plot of the relaxation times τ_d for the dumbbell in the model system with chains of five monomers. All relaxation times have been determined empirically by the requirement $C_d(\tau_d)=0.3$. The parameters T_c and γ obtained from the fits to a power law are reported in Table I. Bottom: Vogel–Fulcher plot of the relaxation times τ_d for the dumbbell in the model system with chains of five monomers. The values of the Vogel temperature T_0 and of the fragility parameter B/T_0 are reported in Table III.

tity, if $C_d(\tau)$ is plotted versus τ/τ_d at different temperatures (for $\tau/\tau_d \geq 0.1$ in the α relaxation regime) close to T_c. Those data can be fitted to the analog of Eq. (4), and if one imposes $b=0.57$ (which resulted from the fit of the data in Fig. 1), one finds an estimate for γ ($\gamma \approx 2.49$) which is reasonably consistent with the value previously found and agrees with the prediction from the MCT exponent relations.

The point which we wish to make in the context of these results is that the observation of the dynamics of the probe molecule suffices to obtain detailed information on the slow dynamics of the matrix. In fact, the relaxation time τ_d extracted in this way yields data for $T_c(N)$ and $T_0(N)$ nicely compatible with the analysis of the data that were presented in sections III and IV, as Fig. 14 demonstrates. In this way, our simulations establish the usefulness of the SMS approach to study the slow dynamics of supercooled liquids. Experimental results[19,20] indicate that the coupling of the probe to transitions in its local environment (which we could identify with metabasin transitions in the supercooled liquid) persists at temperatures close to T_g, where the average dynamics is orders of magnitude slower. We can therefore conjecture that the coupling of the probe dynamics to the matrix dynamics remains qualitatively similar upon lowering T, although we are not able to establish this on a microscopic scale by simulations.

VI. CONCLUSIONS

The present paper has addressed two important questions about the properties of glass forming polymer melts, applying MD simulation methods for the study of a simple coarse-grained bead-spring model of polymer chains.

(i) How do parameters that are useful for the empirical description of the slowing down as the glass transition is approached change when the chain length N is varied, keeping the conditions strictly unchanged in all other respects? Specifically, we addressed quantities such as the critical temperature $T_c(N)$ and exponent $\gamma(N)$ when a power law fit is made to describe the increase in various relaxation times on cooling, as well as the Vogel–Fulcher temperature $T_0(N)$. Since the bead-spring model includes only two basic properties of flexible macromolecules, namely, the connectivity of the chains and the generic feature of all intermolecular interactions, which show dispersion-type attraction at larger distances but excluded-volume type repulsion at short distances, but completely neglects effects of local chain stiffness due to bond bending, and torsional potentials, it is not completely obvious that this model captures correctly subtle features such as these chain length variations.

(ii) The second question that is asked concerns the accuracy of SMS techniques that have recently become rather popular as a local probe of glassy dynamics: Are such local probes sensitive enough that they faithfully "notice" subtle differences in the matrix due to the chain length dependence? The size of a linear dumbbell mimicking a fluorescent probe molecule is rather comparable to the gyration radius of a short oligomer with only $N=5$ (effective) monomers, but it is much smaller than the gyration radius in the case of a chain with $N=25$. This crossover in the size ratio could lead to additional effects, obscuring the pure properties of the matrix.

Although in our study only three short chain lengths ($N=5$, $N=10$, and $N=25$) were available, we nevertheless could obtain rather definitive answers to both questions: (i) the simple, fully flexible, bead-spring model does faithfully reproduce the chain length dependence familiar from the experimental studies (although, of course, the exact form of the N-dependence could not be established from simulations of only three chain lengths), underscoring one more time the high degree of universality of the description of the qualitative properties of glass forming polymers. (ii) These trends can also be extracted rather well from the various relaxation functions and associated relaxation times that one can define (and experimentally measure) for single molecule probes. Our results thus lend additional credence to the reliability of this technique.

We end this discussion with a caveat, however: One should not conclude that our findings imply that the glassy freeze-in of polymer melts is basically understood. In fact, the precise features how the (idealized) MCT breaks down very close to $T_c(N)$, and the precise nature of the slowing down at temperatures lower than $T_c(N)$ clearly have not been elucidated by our study due to excessive demands on computer resources; also the power law describing the breakdown of the Stokes–Einstein relation (cf. Fig. 9) is just an empirical finding, of which an explanation in terms of a microscopic theory is lacking. Moreover while our findings clearly are compatible with ideas such as transitions of the system between various metabasins in phase space, reflecting the dynamic heterogeneity of the glass forming melt, the need to quantify these concepts more precisely remains.

Nevertheless, we hope that our study will encourage more comprehensive experimental and theoretical work on these issues.

ACKNOWLEDGMENTS

Partial support from the Sonderforschungsbereich 625/A3 of the German National Science Foundation and the EU network of excellence SOFTCOMP is acknowledged.

[1] E.-W. Donth, *The Glass Transition. Relaxation Dynamics in Liquids and Disordered Materials* (Springer, Berlin, 2001).
[2] G. Strobl, *The Physics of Polymers* (Springer, Berlin, 1996).
[3] K. Binder, J. Baschnagel, and W. Paul, Prog. Polym. Sci. **28**, 115 (2003).
[4] K. Binder and W. Kob, *Glassy Materials and Disordered Solids: An Introduction to Their Statistical Mechanics* (World Scientific, Singapore, 2005).
[5] I. Gutzov and J. Schmelzer, *The Vitreous State. Thermodynamics, Structure, Rheology and Crystallization* (Springer, Berlin, 1995).
[6] W. E. Moerner and M. Orrit, Science **283**, 1670 (1999).
[7] X.-S. Xie and J. K. Trautmann, Annu. Rev. Phys. Chem. **49**, 441 (1998).
[8] F. Kulzer and M. Orrit, Annu. Rev. Phys. Chem. **55**, 585 (2004).
[9] R. A. L. Vallée, M. Coltet, J. Hofkens, F. C. De Schryver, and K. Müllen, Macromolecules **36**, 7752 (2003).
[10] L. A. Deschenes and D. A. Vanden Bout, J. Phys. Chem. B **106**, 11438 (2002).
[11] N. Tomczak, R. A. L. Vallée, E. M. H. P. van Dijk, M. Garcia-Paragio, L. Kuipers, N. F. van Hulst, and G. J. Vancso, Eur. Polym. J. **40**, 1001 (2004).
[12] A. Schob, F. Cichos, J. Schuster, and C. von Borczyskowski, Eur. Polym. J. **40**, 1019 (2004).
[13] E. Mei, J. Tang, J. M. Vanderkovi, and R. M. Hochstrasser, J. Am. Chem. Soc. **125**, 2730 (2003).
[14] R. M. Dickson, D. J. Norris, and W. E. Moerner, Phys. Rev. Lett. **81**, 5322 (1998).
[15] B. Sick, B. Hecht, and L. Novotny, Phys. Rev. Lett. **85**, 4482 (2000).
[16] A. Lieb, J. M. Zavislan, and L. Novotny, J. Opt. Soc. Am. B **21**, 1210 (2004).
[17] M. Böhmer and J. Enderlein, J. Opt. Soc. Am. B **20**, 554 (2003).
[18] A. P. Bartko, K. Xu, and R. M. Dickson, Phys. Rev. Lett. **89**, 026101 (2002).
[19] R. A. L. Vallée, N. Tomczak, L. Kuipers, G. J. Vancso, and N. F. van Hulst, Phys. Rev. Lett. **91**, 038301 (2003).
[20] R. A. L. Vallée, N. Tomczak, G. J. Vancso, L. Kuipers, and N. F. van Hulst, J. Chem. Phys. **122**, 114704 (2005).
[21] M. Faetti, M. Giordano, D. Leporini, and L. Pardi, Macromolecules **32**, 1876 (1999).
[22] H. Sillescu, J. Non-Cryst. Solids **243**, 81 (1999).
[23] M. D. Ediger, Annu. Rev. Phys. Chem. **51**, 99 (2000).
[24] R. Richert, J. Phys.: Condens. Matter **14**, R703 (2002).
[25] R. A. L. Vallée, M. Van der Auweraer, W. Paul, and K. Binder, Phys. Rev. Lett. **97**, 217801 (2006).
[26] R. A. L. Vallée, M. Van der Auweraer, W. Paul, and K. Binder, Europhys. Lett. **79**, 46001 (2007).
[27] R. A. L. Vallée, W. Paul, and K. Binder, J. Chem. Phys. **127**, 154903 (2007).
[28] P. G. de Gennes, *Scaling Concepts in Polymer Physics* (Cornell University Press, Ithaca, NY, 1979).
[29] P. J. Flory, *Principles of Polymer Chemistry* (Cornell University Press, Ithaca, NY, 1953).
[30] G. Pezzin, F. Zilio-Grande, and P. Sanmartin, Eur. Polym. J. **6**, 1053 (1970) (and references therein).
[31] J. H. Gibbs and E. A. di Marzio, J. Chem. Phys. **28**, 373 (1958).
[32] W. Kauzmann, Chem. Rev. (Washington, D.C.) **43**, 219 (1948).
[33] H.-P. Wittmann, J. Chem. Phys. **95**, 8449 (1991).
[34] M. Wolfgardt, J. Baschnagel, W. Paul, and K. Binder, Phys. Rev. E **54**, 1535 (1996).
[35] See the discussion on p. 324 of Ref. 4.
[36] C. Bennemann, W. Paul, K. Binder, and B. Dünweg, Phys. Rev. E **57**, 843 (1998).
[37] C. Bennemann, J. Baschnagel, W. Paul, and K. Binder, Comput. Theor. Polym. Sci. **9**, 217 (1999).
[38] C. Bennemann, J. Baschnagel, and W. Paul, Eur. Phys. J. B **10**, 323 (1999).
[39] C. Bennemann, W. Paul, J. Baschnagel, and K. Binder, J. Phys.: Condens. Matter **11**, 2179 (1999).
[40] J. Baschnagel, C. Bennemann, W. Paul, and K. Binder, J. Phys.: Condens. Matter **12**, 6365 (2000).
[41] M. Aichele and J. Baschnagel, Eur. Phys. J. E **5**, 229 (2001); **5**, 245 (2001).
[42] J. Buchholz, W. Paul, F. Varnik, and K. Binder, J. Chem. Phys. **117**, 7364 (2002).
[43] J. Baschnagel and F. Varnik, J. Phys.: Condens. Matter **17**, R851 (2005).
[44] W. Paul, *Reviews in Computational Chemistry* (Wiley, New York, 2007), Vol. 25, p. 1.
[45] M. Goldstein, J. Chem. Phys. **51**, 3728 (1969).
[46] F. H. Stillinger and T. H. Weber, Phys. Rev. A **28**, 2408 (1983).
[47] B. Doliwa and A. Heuer, Phys. Rev. Lett. **91**, 235501 (2003).
[48] B. Doliwa and A. Heuer, Phys. Rev. E **67**, 030501 (2003).
[49] M. Vogel, B. Doliwa, A. Heuer, and S. C. Glotzer, J. Chem. Phys. **120**, 4404 (2004).
[50] R. A. Denny, D. R. Reichman, and J.-P. Bouchaud, Phys. Rev. Lett. **90**, 025503 (2003).
[51] L. Angelani, G. Ruocco, M. Sampoli, and F. Sciortino, J. Chem. Phys. **119**, 2120 (2003).
[52] J. Kim and T. Keyes, J. Chem. Phys. **121**, 4237 (2004).
[53] D. Coslovich and G. Pastore, Europhys. Lett. **75**, 784 (2006).
[54] G. A. Appignanesi, J. A. Rodrigues Fris, R. A. Montani, and W. Kob, Phys. Rev. Lett. **96**, 057801 (2006).
[55] W. Götze and L. Sjögren, Rep. Prog. Phys. **55**, 241 (1992).
[56] J. Jäckle, Rep. Prog. Phys. **49**, 171 (1986).
[57] P. G. Debenedetti, *Metastable Liquids* (Princeton University Press, Princeton, 1977).
[58] H. Vogel, Phys. Z. **22**, 645 (1921); G. S. Fulcher, J. Am. Ceram. Soc. **8**, 339 (1925).
[59] The software package OCTA (http://octa.jp) was used.
[60] *Monte Carlo and Molecular Dynamics of Condensed Matter*, edited by K. Binder and G. Ciccotti (Societa Italiana di Fisica, Bologna, 1996).
[61] W. Paul, Chem. Phys. **284**, 59 (2002).
[62] F. Stickel, E. W. Fischer, and R. Richert, J. Chem. Phys. **104**, 2043 (1996).
[63] A. Barbieri, E. Campani, S. Capaccioli, and D. Leporini, J. Chem. Phys. **120**, 437 (2004).
[64] A. Ottochian, D. Molin, A. Barbieri, and D. Leporini, J. Chem. Phys. **131**, 174902 (2009).
[65] M. F. Gelin and D. S. Kosov, J. Chem. Phys. **125**, 054708 (2006).
[66] C.-Y. Lu and D. A. Vanden Bout, J. Chem. Phys. **125**, 124701 (2006).